MD Med Discoveries

An open access journal of science and medicine

Tripterygium Wilfordii Reduces the Inflammatory Response in Transplant Vasculopathy

Qimin Wang[1]; Yanqing Su[2]; Yang Ye[1]; Yao Lu[3]*

[1]*Department of Cardiovascular Surgery, Union Hospital Affiliated to Fijian Medical University, Fuzhou, Fujian, 350001, China.*

[2]*Department of Pharmacy, Xiamen Children's Hospital, Xiamen, 361006, Fujian, China.*

[3]*Hebei Provincial Hospital of Traditional Chinese Medicine, Shijiazhuang, Hebei, 050011, China.*

*Corresponding Author: Yao Lu

Tel: 86-13365917109; Email: 2383217518@qq.com

Abstract

Background: Transplant vasculopathy (TV) is the most challenging threat during organ transplantation. The pathological induction of TV results from vascular endothelial cell injury. This study established the in vitro model of TV and investigated the attenuating effect of triptolide (TPL) on TV through multiple in vitro and in vivo assays.

Methods: The inflammation model was established by stimulating rat vascular endothelial cells with lipopolysaccharides (LPS). Rat vascular endothelial cells were isolated, cultured, and characterized as CD31-positive. For in vivo assays, Wistar and Sprague–Dawley rats were divided into S-S, W-S and W-S-TPL groups. The transplanted arteries were harvested at 1,4, and 8 weeks post-operation.

Results: After LPS treatment, the cell viability was significantly reduced, and the IL-1β and TNF-α levels were significantly elevated, indicating that the LPS-induced in vitro inflammation model was successfully constructed. Nevertheless, the changes in the expression of inflammatory factors and vascular adhesion molecules, as well as the p-p65 levels, which were triggered by LPS, were significantly mitigated upon the stimulation of TPL. Results from rat models showed that intimal thickening was observed in the W-S group and significantly reduced in the TPL-treated group a week after transplantation. Consistent with the in vitro data, VCAM-1, ICAM-1, p-p38, and p-p65 expression was significantly attenuated in the TPL-treated group compared with the W-S group.

Conclusions: This work confirmed that TPL may alleviate the progression of allograft vasculopathy and reduce the inflammation process by inhibiting the phosphorylation of p65 and p38, which are the key protein of the NF-κB and MAPK pathway, respectively.

Keywords: Transplant vasculopathy; Triptolide; Intima thickness; Adhesion molecule.

Introduction

Organ transplantation is widely applied in clinical practice. Due to the accelerated improvement of surgical techniques and the effective application of immunosuppressive agents, the success rate of organ transplantation has been greatly enhanced [1]. However, these measures failed to effectively improve the status of long-term graft survival. Therefore, prolonging the survival time of transplanted organs remains difficult to address in the field of organ transplantation. Loss of graft function due to chronic rejection is a major cause of organ transplant failure in clinical practice [2]. Long-term follow-up clinical data suggested that transplant vasculopathy (TV) occurs in approximately 90% of allografts [3]. TV is a severe vascular intimal proliferative lesion that may affect the entire length of the graft, leading to late arterial stenosis, occlusion, and ultimately graft ischemia and transplantation failure [4].

The occurrence of TV results from various pathophysiological mechanisms. Not only non-immune factors such as organ preservation, ischemia-reperfusion injury, infection and donor hypertension, age, and sex matching are involved in TV, but immune factors such as antibody and cell-mediated immune rejection, donor-specific antibody production, and inflamma-

tory cytokines produced by innate immune cells such as macrophages are also related to the development of TV [3,5]. These factors are interrelated, and eventually lead to the initiation of TV. Moreover, TV has similar clinical pathological changes to most common cardiovascular diseases in clinical practice, such as atherosclerosis and vascular restenosis after surgical treatment, which were mainly manifested as perivascular inflammatory cell infiltration, smooth muscle cell proliferation, vascular intimal thickening, neointima formation, and finally causing graft stenosis or even vascular occlusion [6]. However, unique pathological characteristics were indicated during the development of TV. Unlike atherosclerotic lesions, which present local eccentric uneven distribution as its pathological characteristic, TV lesions are characterized by diffused involvement of the entire length of the graft [7]. Since the existence of the aforementioned multiple biological factors for the development of TV, effective strategies for simultaneously controlling those signaling pathways have not been elucidated.

In recent years, the clinical significance of traditional Chinese medicine (TCM) has been underlined by domestic and foreign researchers, especially in the field of anti-transplant immune rejection. Because of their pharmacological and biological effects, many traditional Chinese medicines have been applied in clinical practice. Tripterygium wilfordii Hook F is a common medicinal herb in TCM, and its efficacy in the treatment of inflammatory and autoimmune diseases was confirmed after long-term research [8]. The main component of T. wilfordii Hook F is triptolide (TPL), a diterpene lactone widely identified in the said herb. Results from a mouse xenograft model have shown that TPL attenuates the survival of pancreatic tumor cells [9]. Other studies have shown that TPL has immunosuppressive effects and can significantly prolong organ postoperative survival [10]. Given the broad immunosuppressive and antiproliferative effects mediated by TPL, we used in vitro assays and in vivo rat aortic transplantation models to assess the effect of TPL on attenuating TV and unveiled the underlying molecular mechanisms.

Materials and methods

Cell culture and treatment: Primary vascular endothelial cells isolated from Sprague–Dawley (SD) rats were purchased from Xiamen Immocell Biotechnology Co.,Ltd. (Xiamen), and cultured in Dulbecco's Modified Eagle's Medium (DMEM) containing 10% fetal bovine serum (FBS) and 100 U/mL penicillin and 100 μg/mL streptomycin at 37°C with 5% CO_2. Cells were seeded 24 h before exposure to various concentrations of lipopolysaccharide (LPS; 1, 5, 10, and 20 μg/mL) and TPL (0, 5, 10, 20, and 30 nmol/L) for 2 h.

ELISA: The expression of interleukin-1β (IL-1β) and tumor necrosis factor α (TNF-α) was determined by an ELISA kit (Krishgen Biosystems, USA) following the manufacturer's instructions.

MTT assay: For the MTT assay, 2×10^3 rat aortic epidermal cells were plated in 96-well plates and kept in the incubator overnight for attachment. The medium was substituted with fresh ones without FBS, and cells were pretreated with different concentrations of LPS and TPL for 2 h prior to treatment with 150 μmol/L H_2O_2 overnight. Afterwards, 20 μL of MTT (3[4,5-dimethylthiazol-2-yl]-2,5- diphenyl-tetrazolium bromide) dissolved in PBS solution was added to each well, and the cells were cultured at 37°C for another 4 h. Subsequently, 200 μL of dimethyl sulfoxide (DMSO) was added to each well to release the colored formazan in viable cells. Finally, the absorbance was measured at 570 nm using a microplate reader.

Flow cytometry: Rat aortic endothelial cells (1×10^6 cells) were plated in 6-well plates and incubated for 24 h in various doses of LPS and TPL, after which FITC labeled Annexin V (200 μg/mL) and propidium iodide (30 μg/mL; A211-02, Vazyme) were added to cells and kept at room temperature for 10 min. Subsequently, the fluorescent signals indicating the apoptotic cell percentage were quantified using the NovoCyte flow cytometer.

Animal and treatment: Healthy male adult and clean grade Wistar and SD rats (between 120 g and 150 g) (Shanghai SLAC Laboratory Animal Co., Ltd.) were used as donors. SD rats (250–300 g) were used as recipients (Shanghai SLAC Laboratory Animal Co., Ltd). Abdominal aortic transplantation was performed following a previously described procedure [11]. The 10-15 mm infrarenal abdominal aortic segments of donors were isolated, excised, and replaced with the recipients' infrarenal abdominal aortic segments by end-to-end anastomosis using 12-0 monofilament nylon sutures (Shanghai Pudong Jinhuan Medical Supplies Co. Ltd., No. 20192650812) under an operating microscope. All procedures were performed under methoxyflurane inhalation anesthesia (Shanghai Second Pharmaceutical Factory, No. 910610). Technical success was defined as no graft occlusion within 10 days post-transplantation. The success rate of graft was more than 90%.

In this study the rats were subdivided into three groups: SD rats as both donors and recipients (S-S), Wistar rats as donors and SD rats as recipients (W-S), and TPL treatment after vascular graft (W-S-TPL). After transplantation, in the W-S-TPL group, TPL (0.5 mg/kg) was subcutaneously injected every other day until the endpoint of the experiment (8 weeks post-transplantation). The W-S group received an equal amount of saline subcutaneously. No extra immunosuppressive drugs were utilized in any group. Grafts were harvested at 8 weeks under anesthesia. Tissues were sectioned at 4 μm thickness, and then deparaffinized and rehydrated.

Immunohistochemistry: After the sections were deparaffinized and rehydrated, they were incubated with antibodies against VCAM-1(CAT: ab174279, 1:2,000, Abcam, Shanghai, China) and ICAM-1 (CAT: ab109361, 1:1,500, Abcam, Shanghai, China) at 4°C overnight. Then, the samples were incubated with anti-rabbit IgG/horse radish peroxidase (HRP) for 1 h at 37°C. The average optical density (AOD) representing the expression of VCAM-1, ICAM-1, and p-p65 was quantified by ImageJ software.

Ethics statement: All animal experiments were conducted in strict compliance with the Ministry of Animal Experiments and approved by the ethics committee of the Academy of Integrative Medicine, Fujian University of Traditional Chinese Medicine. The animals were housed under specific pathogen-free conditions at the Key Laboratory of Integrative Medicine of Fujian Province University, Fujian University of Traditional Chinese Medicine and were handled by trained personnel in accordance with the Guide for the Care and Use of Laboratory Animals (National Institutes of Health publication no. 80-23, revised 1996).

Western blotting: Cells were lysed using the RIPA buffer and total protein concentrations were determined using a bicinchoninic acid assay kit (Thermo Fisher Scientific). Equal amounts of lysates were separated by 10% SDS-PAGE gels. Then, the proteins were transferred onto a polyvinylidene difluoride mem-

brane at 4°C for 2 h. The blots were then blocked by incubating them with 5% non-fat milk dissolved in tris-buffered saline with Tween 20 (TBST) buffer for 1 h. Afterwards, the membranes were incubated with the corresponding first antibodies at 4°C for 16 h, washed three times with TBST, and incubated with HRP anti-rabbit IgG (H+L) (CAT: SA00001-2, 1:10,000, Proteintech, Wuhan, China) at room temperature for 2 h. Subsequently, the blots were washed thrice, and the signals were captured by a Chemiluminescent Detection kit (Thermo Fisher Scientific). Antibodies were listed as follows: VCAM-1 (CAT: ab174279, 1:2,000, Abcam, Shanghai, China), ICAM-1 (CAT: ab109361, 1:1,500, Abcam, Shanghai, China), p-p65 (CAT: ab76302, 1:1,000, Abcam, Shanghai, China), p65 (CAT: 10745-1-AP, 1:2,000, Proteintech, Wuhan, China), p-p38 (CAT: 28796-1-AP, 1:2,000, Proteintech), p38 (CAT: 14064-1-AP, 1:2,000, Proteintech), beta actin (CAT: 20536-1-AP, 1:2,000, Proteintech), and GAPDH (CAT: 10494-1-AP, 1:3,000, Proteintech, Wuhan, China).

Quantitative real-time PCR (RT-qPCR)

Total RNA was extracted from the cells using the Total RNA Extraction kit (Vazyme). Next, the cDNA was synthesized using a HiScript II 1st Strand cDNA Synthesis Kit (Vazyme), following the manufacturer's instructions. Subsequently, the ChamQ SYBR qPCR Master Mix (Vazyme) was utilized for the real time PCR on an iQ5 Real-Time PCR Detection System (Bio-Rad). Triplicates were included in all groups. The qPCR primer pairs used were as follows:

18S rRNA forward primer: 5'-AGGCGCGCAAATTACCCAATCC-3', 18S rRNA reverse primer: 5'-GCCCTCCAATTGTTCCTCGTTA-AG-3'; VCAM-1 forward primer: 5'-TGATGTTCAAGGAAGAGA-3', VCAM-1 reverse primer: 5'-TGGCAGGTATTATTAAGGA-3'; ICAM-1 forward primer: 5'-CAAGAAGATAGCCAACCAATGTG-3', ICAM-1 reverse primer: 5'-GGAGTCCAGTACACGGTGA-3'.

Association of TPL with biological signaling pathways and disease

The chemical constituents of TPL were screened in TCMSP and ETCM databases, and the target genes of rejection disease after heart transplantation were searched through DisGeNET and Drugbank databases. Among them, TPL contains 61 active ingredients, 180 drug genes, and a total of 8782 disease target genes. There are 21 intersection genes between TPL and rejection after heart transplantation. The David database was used to predict 145 KEGG pathways. Cytoscape 3.2.1 software was used to predict the TOP10 core intersection genes ranked by Degree value.

Statistical analysis: Data was analyzed on SPSS version 20.0, and all parametric data were expressed as mean ± standard deviation. Statistical significance was set at $p<0.05$. All the comparisons between two groups were performed using the Student's t-test.

Results

Characterization of an in vitro inflammation model by treating aortic endothelial cells with LPS: To establish an LPS-triggered inflammation model, we started by isolating the rat aortic endothelial cells from SD rats via collagenase digestion. The extracted cells were then imaged using a differential interference contrast microscope (Figure 1A). The morphology of isolated endothelial cells was homogenous. To determine the cells at the molecular level, the aortic endothelial cells were stained with anti-CD31 antibodies. Subsequently, the expression of cell surface antigen was analyzed by flow cytometry, and isotype antibody was used as a control. The results from flow cytometry analysis indicated that CD31, the marker for endothelial cells, but not the isotype control, was highly expressed on the cell surface of these cells, confirming that the cells were endothelial cells (Figure 1B). Next, we tried various concentrations of LPS to construct an in vitro cellular inflammation model. The MTT assay showed that the increasing LPS concentrations significantly decreased the viability of endothelial cells (Figure 1C). Moreover, the viability of endothelial cell was inhibited by approximately 50% at 10 µg/mL LPS stimulation, and this concentration was selected for the following experiments (Figure 1C). Furthermore, the expression of proinflammatory cytokines in endothelial cells was quantified by ELISA. We found that the levels of inflammatory cytokines IL-1β and TNF-α were dramatically increased upon the treatment of LPS ($p<0.0001$). Collectively, our results revealed that high-quality rat aortic endothelial cells were isolated, and an in vitro inflammation model was successfully constructed.

TPL inhibits apoptosis and reduces the levels of inflammatory factors: To investigate the suppressive effects of TPL on the LPS-induced inflammatory response in aortic endothelial cells, different concentrations of TPL were used to treat cells. We observed that TPL attenuated the proliferation mitigation directed by LPS in a dose-dependent manner (Figure 2A). TPL began to exert a protective effect on cells at 10 nmol/L and significantly increased cell viability at 30 nmol/L (Figure 2A). Thus, 30 nmol/L of TPL was chosen as the concentration in subsequent experiments (Figure 2A). In addition, flow cytometry results showed that LPS induced cell death, including both early and late apoptosis, while TPL significantly decreased the proportion of apoptotic cells (Figure 2B, 2C). Moreover, the increased levels of inflammatory factors IL-1β and TNF-α triggered by LPS were dramatically reduced after TPL treatment (Figure 2D).

TPL regulates the expression of inflammation-induced endothelial adhesion molecules: It is reported that during inflammation, local innate cells release cytokines and vasoactive factors that induce the activation of endothelial cells by increasing the permeability and upregulating adhesion molecules expression (i.e., ICAM-1 and VCAM-1). The RT-qPCR results indicated that LPS treatment resulted in a significant elevation of ICAM-1 and VCAM-1 in endothelial cells, while TPL clearly decreased the increase of these factors (Figure 3A, 3B). In addition, western blotting yielded the same results (Figure 3C). We also found that the reduction of adhesion molecule levels by TPL might be related to the reduction of the NF-κB pathway by decreasing the phosphorylation level of p65 (Figure 3C-F). These findings show that the LPS can induce adhesion molecules expression, which could be alleviated by TPL treatment.

TPL decreases LPS-induced neointimal thickness and the expression of VCAM-1, ICAM-1, and p-p65: Aortic transplantation was performed to study the effect of TPL on transplantation using an in vivo model. The intimal thickness in the W-S group increased dramatically after one week of vascular transplantation and decreased significantly after the treatment of TPL sustained-release medication (Figure 4A). Immunohistochemistry analysis demonstrated that after vascular graft, the AOD of VCAM-1 and ICAM-1 was drastically increased compared with that of the controls (Figure 4B). However, after TPL treatment, the increased protein expression was significantly alleviated upon TPL stimulation (Figure 4B).

TPL has the potential to regulate MAPK and NF-κB signaling
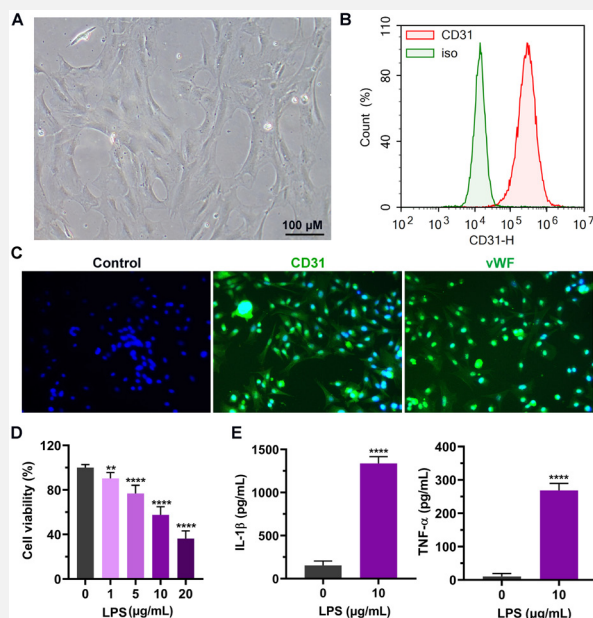
**Figure 1:** LPS induces inflammation in rat aortic endothelial cells.
A. Representative image of the rat aortic endothelial cells (scale bar = 100 μm).
B. Isolated cells were stained with CD31 and isotype-matched antibody for flow cytometry analysis.
C. Immunohistochemical staining of endothelial cell markers CD31 and von Willebrand factor (vWF).
D. After rat aortic endothelial cells were incubated with different concentrations of LPS, the cell activity was detected by MTT assay.
E. After the cells were treated with 10 μg/mL LPS, the contents of IL-1β and TNF-α in the cell culture supernatant were detected by ELISA.
Three independent experiments were carried out and graph data are expressed as means ± standard deviation **p<0.01, ****p<0.0001.
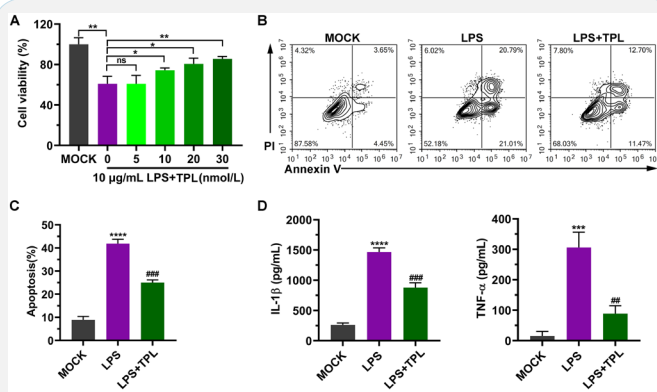
Figure 2: TPL ameliorates LPS-induced apoptosis and inflammatory factor release.
A. After aortic endothelial cells were treated with 10 μg/mL LPS and different concentrations of Tripterygium wilfordii (TPL), cell viability was measured by MTT.
B. After cells were treated with 10 μg/mL LPS and 30 nmol/L Tripterygium wilfordii (TPL), analysis of apoptosis was performed by flow cytometry. Signals in the low right quadrant (Annexin V+/PI-) represent early apoptotic cells, and signals in the upper right quadrant (Annexin V+/PI+) represent late apoptotic cells.
C. Statistics of apoptotic cells.
D. ELISA was used to detect the expression levels of IL-1β and TNF-α.
Graph data are expressed as means ± standard deviation from three independent experiments.
LPS vs. MOCK, ns, not significant, *p<0.05, **p<0.01, ***p<0.001, ****p<0.0001. LPS vs. TPL, ## p<0.01, ### p<0.001.
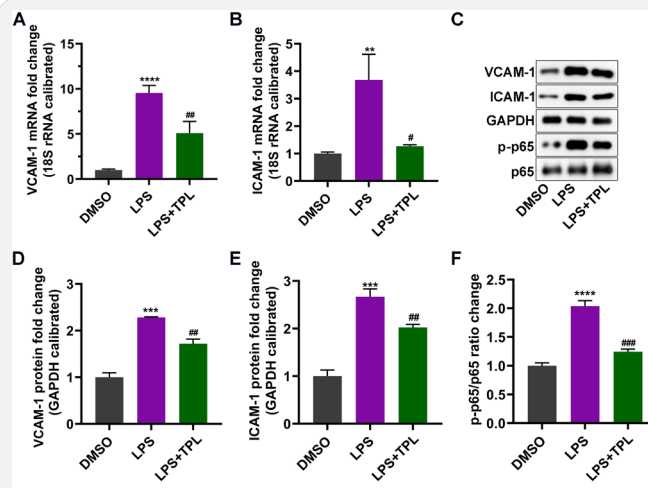

Figure 3: Effects of TPL on the expression of endothelial adhesion molecules.
Cells were treated with 10 μg/mL LPS and 30 nmol/L Tripterygium wilfordii (TPL).
A-B. VCAM-1 and ICAM-1 mRNA expression was detected by RT-qPCR.
C. The protein expression of VCAM-1, ICAM-1, and p-p65 was determined by Western blotting.
D-F. The statistical results of the protein expression densitometric analysis. Data was expressed as mean ± standard deviation. n=3 in each group. DMSO vs. LPS, **p<0.01, ***p<0.001, ****p<0.0001. LPS vs. TPL, #p<0.05, ##p<0.01, ###p<0.001.
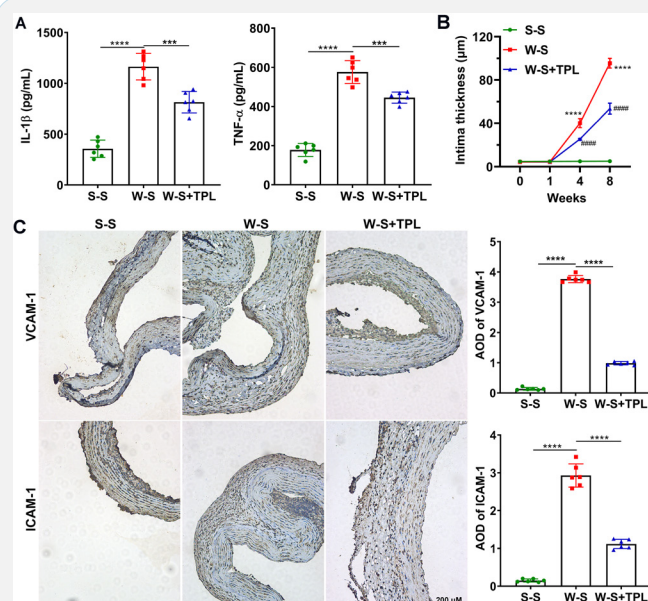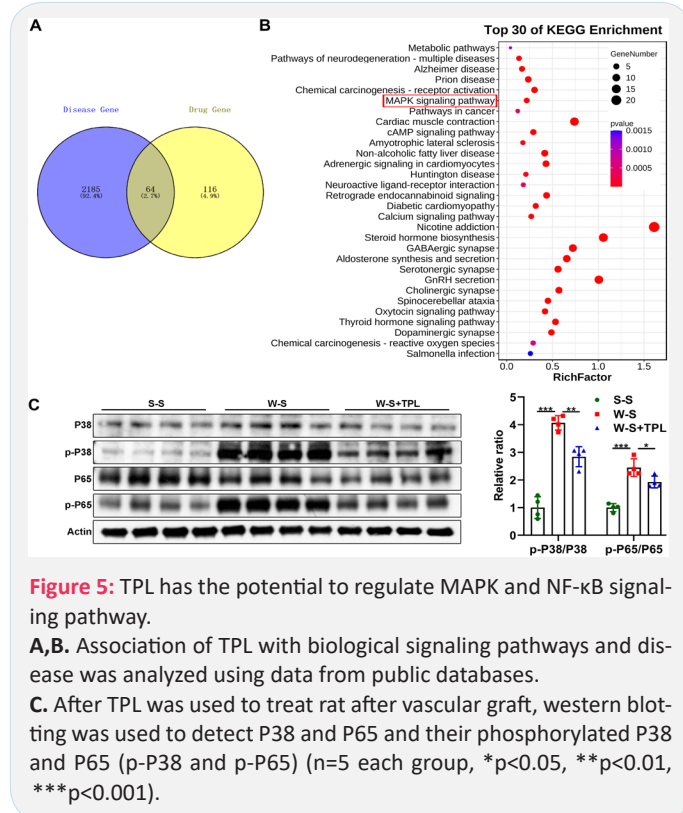

Figure 4: TPL decreases LPS-induced neointimal thickness and the expression of VCAM-1 and ICAM-1.
TPL was used to treat rat after vascular graft.
A. The contents of IL-1β and TNF-α in rat plasma were detected by ELISA.
B. Quantitative results of intimal thickness (n=5 each group, W-S vs. S-S, ****p<0.0001. W-S vs. W-S-TPL, ####p<0.0001).
C. Left: Representative immunohistochemical images of aortic sections of each group (scale=200 μm). Right: Average optical density (AOD) of VCAM-1 and ICAM-1 analyzed by immunohistochemistry at 8 weeks after vascular graft (n=5 each group, ****p<0.0001).

Figure 5: TPL has the potential to regulate MAPK and NF-κB signaling pathway.

A,B. Association of TPL with biological signaling pathways and disease was analyzed using data from public databases.

C. After TPL was used to treat rat after vascular graft, western blotting was used to detect P38 and P65 and their phosphorylated P38 and P65 (p-P38 and p-P65) (n=5 each group, *p<0.05, **p<0.01, ***p<0.001).

pathway: The association between TPL and signaling pathways or diseases was analyzed using data from public databases, and it was found that TPL may be involved in the regulation of MAPK signaling pathway (Figure 5A and 5B). After TPL was used to treat rat after vascular graft, the ratio of p-P38/P38 and p-P65/P65 was reduced (Figure 5C). These findings revealed that TPL has the potential to regulate MAPK and NF-κB signaling pathway.

Discussion

Pathological hallmarks of TV include the development of marked inflammation in vessel walls, neointima formation, and progressive luminal obstruction [12]. TV limits the function and long-term survival of organs and is an urgent problem to be solved in the field of organ transplantation [13]. In this study, we analyzed the role and molecular mechanism of TPL in the development of TV using in vitro and rat arterial transplantation models.

In the present research, we observed that LPS induced inflammation in rat vascular endothelial cells, which is indicated by the significantly elevated IL-1β and TNF-α expression, as well as inhibited cell viability. However, the TPL treatment can significantly reduce inflammatory factor expression, increase cell viability, reduce the rate of apoptosis, and reduce VCAM-1, ICAM-1, and p-p65 expression. Cytokines also play a role in this related vascular remodeling, which is a complex process carried out by the body in response to various stimulating factors and microenvironment. Moreover, this process is involved in various cytokines and adhesion molecules [14]. IL-1β belongs to the IL-1 family and promotes inflammatory response and angiogenesis [15]. Multiple pathways mediated by TNF-α may cause dysfunction of vascular endothelial cells. Among these pathways, TNF-α was found to bind to endothelial adhesion molecules to activate the NF-κB pathway [16]. TNF-α also activates endothelial cells, increases the adhesion ability of endothelial cells, and improves the ability of cellular vascular infiltration [17]. During the development of acute rejection and allograft vasculopa-

thy, endothelial cells can highly express adhesion molecules (ICAM-1, VCAM-1) and E/P-selectin [18]. E/P-selectin recruits circulating leukocytes by binding certain glycoprotein sialidase X on the surface of leukocytes. While ICAM-1 binds to lymphoid function-associated antigens and macrophage antigens on the surface of leukocytes, VCAM-1 is a very late antigen that binds to the surface of monocytes [19]. Dietrich et al. demonstrated that in the ICAM-1$^{-/-}$ transplantation model, acute rejection was significantly reduced, and the degree of development of graft vasculopathy was attenuated [20]. In our study, we found that LPS induced the upregulation of proinflammatory factors and adhesion molecules, while TPL reversed this phenomenon. These results suggest that TPL slows the development of TV to some extent.

TPL has significant anti-inflammatory, immunosuppressive, and antitumor effects [21]. Studies have shown that TPL can reduce the expression of the apoptotic gene bcl-2 and increase the expression of pro-apoptotic Bax expression, thereby inducing cell apoptosis [22]. Hachida et al. found that TPL significantly reduces the atherosclerosis of vascular bridges by inhibiting the neointimal formation of vascular bridges in mice receiving allogeneic heart transplantation by decreasing the expression of PDGF-A [23]. Luo et al. proposed that TPL may inhibit vascular intimal thickening by inhibiting IFN-γ [24].

The results from the xenograft rat vascular transplantation model revealed that p-p65 and p-p38 expression was abnormally increased, which was accompanied with vascular intimal hyperplasia and luminal narrowing, which suggested that p-p65 and p-p38 may be involved in the occurrence and development of allograft vasculopathy. Thus, p-p65 and p-p38 may serve as a new indicator for evaluating the level of allograft vasculopathy. TPL also effectively alleviated the development of vascular intimal lesions in allograft vasculopathy and significantly reduced p-p65 expression. Because phosphorylation of p65 and p38 are critical steps in the activation of NF-κB and MAPK signaling, respectively, we concluded that TPL may alleviate the progression of vascular lesions in allografts by inhibiting the NF-κB and MAPK pathways. Studies have shown that NF-κB inhibitors have preventive efficacy against TV, but high-dose immunosuppressive agents have great side effects on the receptor [25]. TPL can exert pharmacological effects on tumorigenesis, inflammation, immunosuppressive, renal/cardio protection, and abnormal angiogenesis [26].

This study also has some limitations. TPL has a wide range of effects, and the rejection of transplanted organs has not been specifically verified. Thus, the mechanism should be investigated further. In addition, we have not deeply explored the toxicity and side effects of TPL. A future study will take these points as the focus of exploration.

Conclusions

In conclusion, we found that TPL may have some alleviating effect on TV by reducing the expression of inflammatory factors and vascular adhesion molecules, suggesting that TPL may have important clinical value as a potential therapeutic agent to prevent TV and improve the long-term survival rate of grafts.

Declarations

Ethics approval and consent to participate: The study was approved by the ethics committee of the Academy of Integrative Medicine, Fujian University of Traditional Chinese Medicine.

References

1. Shi BY, Liu ZJ, Yu T. Development of the organ donation and transplantation system in China. Chinese medical journal. 2020; 133(7): 760-5.

2. Waki K, Terasaki PI, Kadowaki T. Long-term pancreas allograft survival in simultaneous pancreas-kidney transplantation by era: UNOS registry analysis. Diabetes care. 2010; 33(8): 1789-91.

3. Luo Z, Liao T, Zhang Y, Zheng H, Sun Q, Han F, et al. Triptolide Attenuates Transplant Vasculopathy Through Multiple Pathways. Frontiers in immunology. 2020; 11: 612.

4. Wang Y, Zhao D, Sheng J, Lu P. Local honokiol application inhibits intimal thickening in rabbits following carotid artery balloon injury. Molecular medicine reports. 2018; 17(1): 1683-9.

5. Sucher R, Rademacher S, Jahn N, Brunotte M, Wagner T, Alvanos A, et al. Effects of simultaneous pancreas-kidney transplantation and kidney transplantation alone on the outcome of peripheral vascular diseases. BMC nephrology. 2019; 20(1): 453.

6. Watanabe T, Seguchi O, Yanase M, Fujita T, Murata Y, Sato T, et al. Donor-Transmitted Atherosclerosis Associated With Worsening Cardiac Allograft Vasculopathy After Heart Transplantation: Serial Volumetric Intravascular Ultrasound Analysis. Transplantation. 2017; 101(6): 1310-9.

7. Sun X, Li S, Gan X, Chen K, Yang D, Yang Y. NF2 deficiency accelerates neointima hyperplasia following vascular injury via promoting YAP-TEAD1 interaction in vascular smooth muscle cells. Aging. 2020; 12(10): 9726-44.

8. Su D, Song Y, Li R. [Comparative clinical study of rheumatoid arthritis treated by triptolide and an ethyl acetate extract of Tripterygium wilfordii]. Zhong xi yi jie he za zhi = Chinese journal of modern developments in traditional medicine. 1990; 10(3): 144-6,31.

9. Chugh R, Sangwan V, Patil SP, Dudeja V, Dawra RK, Banerjee S, et al. A preclinical evaluation of Minnelide as a therapeutic agent against pancreatic cancer. Science translational medicine. 2012; 4(156): 156ra39.

10. Li H, Li L, Mei H, Pan G, Wang X, Huang X, et al. Antitumor properties of triptolide: phenotype regulation of macrophage differentiation. Cancer biology & therapy. 2020; 21(2): 178-88.

11. Koulack J, McAlister VC, Giacomantonio CA, Bitter-Suermann H, MacDonald AS, Lee TD. Development of a mouse aortic transplant model of chronic rejection. Microsurgery. 1995; 16(2): 110-3.

12. Nichols JE, Niles J, Riddle M, Vargas G, Schilagard T, Ma L, et al. Production and assessment of decellularized pig and human lung scaffolds. Tissue engineering Part A. 2013; 19(17-18): 2045-62.

13. Chen H, Ambadapadi S, Wakefield D, Bartee M, Yaron JR, Zhang L, et al. Selective Deletion of Heparan Sulfotransferase Enzyme, Ndst1, in Donor Endothelial and Myeloid Precursor Cells Significantly Decreases Acute Allograft Rejection. Scientific reports. 2018; 8(1): 13433.

14. Qi D, Wei M, Jiao S, Song Y, Wang X, Xie G, et al. Hypoxia inducible factor 1α in vascular smooth muscle cells promotes angiotensin II-induced vascular remodeling via activation of CCL7-mediated macrophage recruitment. Cell death & disease. 2019; 10(8): 544.

15. Zhang S, Cheng M, Wang Z, Liu Y, Ren Y, Rong S, et al. Secoisolariciresinol Diglucoside Exerts Anti-Inflammatory and Antiapoptotic Effects through Inhibiting the Akt/IκB/NF-κB Pathway on Human Umbilical Vein Endothelial Cells. Mediators of inflammation. 2020; 2020: 3621261.

16. Cui S, Men L, Li Y, Zhong Y, Yu S, Li F, et al. Selenoprotein S Attenuates Tumor Necrosis Factor-α-Induced Dysfunction in Endothelial Cells. Mediators of inflammation. 2018; 2018: 1625414.

17. Yoshimatsu Y, Kimuro S, Pauty J, Takagaki K, Nomiyama S, Inagawa A, et al. TGF-beta and TNF-alpha cooperatively induce mesenchymal transition of lymphatic endothelial cells via activation of Activin signals. PloS one. 2020; 15(5): e0232356.

18. Styles JN, Converse RR, Griffin SM, Wade TJ, Klein E, Nylander-French LA, et al. Human Cytomegalovirus Infections Are Associated With Elevated Biomarkers of Vascular Injury. Frontiers in cellular and infection microbiology. 2020; 10: 334.

19. Zhou Q, Sun HJ, Liu SM, Jiang XH, Wang QY, Zhang S, et al. Anti-inflammation effects of the total saponin fraction from Dioscorea nipponica Makino on rats with gouty arthritis by influencing MAPK signalling pathway. BMC complementary medicine and therapies. 2020; 20(1): 261.

20. Dietrich H, Hu Y, Zou Y, Dirnhofer S, Kleindienst R, Wick G, et al. Mouse model of transplant arteriosclerosis: role of intercellular adhesion molecule-1. Arteriosclerosis, thrombosis, and vascular biology. 2000; 20(2): 343-52.

21. Shao H, Ma J, Guo T, Hu R. Triptolide induces apoptosis of breast cancer cells via a mechanism associated with the Wnt/β-catenin signaling pathway. Experimental and therapeutic medicine. 2014; 8(2): 505-8.

22. Chen T, Zhao X, Ren Y, Wang Y, Tang X, Tian P, et al. Triptolide modulates tumour-colonisation and anti-tumour effect of attenuated Salmonella encoding DNase I. Applied microbiology and biotechnology. 2019; 103(2): 929-39.

23. Hachida M, Lu H, Zhang X, Saito S, Furutani Y, Matsuoka R, et al. Inhibitory effect of triptolide on platelet derived growth factor-A and coronary arteriosclerosis after heart transplantation. Transplantation proceedings. 1999; 31(7): 2719-23.

24. Govender L, Mikulic J, Wyss JC, Gaide O, Thome M, Golshayan D. Therapeutic Potential of Targeting Malt1-Dependent TCR Downstream Signaling to Promote the Survival of MHC-Mismatched Allografts. Frontiers in immunology. 2020; 11: 576651.

25. Zhou K, Chang Y, Han B, Li R, Wei Y. MicroRNAs as crucial mediators in the pharmacological activities of triptolide (Review). Experimental and therapeutic medicine. 2021; 21(5): 499.

26. Zhou K, Chang Y, Han B, Li R, Wei Y. MicroRNAs as crucial mediators in the pharmacological activities of triptolide (Review). Experimental and Therapeutic Medicine. 2021; 21(5).